Check for updates

High nuclearity structurally – related Mn supertetrahedral T4 aggregates†

Katerina Skordi,[a] Antonis Anastassiades,[a] Adeline D. Fournet,[b] Rahul Kumar,[b]
Michael Schulze, [ID][c] Wolfgang Wernsdorfer, [ID][c] George Christou, [ID][b]
Vassilios Nastopoulos, [ID][d] Spyros P. Perlepes, [ID][d]
Constantina Papatriantafyllopoulou [ID]*[e] and Anastasios J. Tasiopoulos [ID]*[a]

The simultaneous employment of 1,3-propanediol and di-2-pyridyl ketone in Mn carboxylate chemistry has provided access to three new, structurally-related [Mn$_{24}$] and [Mn$_{23}$] clusters. They are based on nanosized supertetrahedal T4 Mn/O structural cores and exhibit slow relaxation of magnetization below 3.5 K.

High nuclearity metal clusters of paramagnetic 3d metal ions have attracted immense research interest over the past few decades due to their fascinating crystal structures (unprecedented metal topologies and nuclearities), and intriguing magnetic properties, such as single molecule magnetism behaviour and/or abnormally high ground state spin values.[1–11] In addition, they are sometimes structural models of well–known metal complexes existing in nature, for example oligonuclear Mn clusters are structural models of the oxygen-evolving Mn complex located in the active site of Photosystem II.[12] More recently, several polynuclear compounds have been reported to exhibit similar structures to a series of inorganic solids including various oxides/hydroxides,[13–16] chalcogenides,[17–20] halides,[21] polyoxometallates,[22–24] perovskites,[25] and others.

Among them, the supertetrahedral metal – chalcogenide clusters which are exact fragments of the zinc blende type of lattice have attracted significant attention.[26–28] Such compounds, denoted as T_n (n = 2, 3, 4, . . .), consist of four, ten,

[a] *Department of Chemistry, University of Cyprus, Nicosia 1678, Cyprus.*
   E-mail: atasio@ucy.ac.cy
[b] *Department of Chemistry, University of Florida, Gainesville, Florida 32611-7200,*
   USA
[c] *Institute of Quantum Materials and Technologies (IQMT),*
   Hermann-von-Helmholtz-Platz 1, Eggenstein-Leopoldshafen, 76344, Germany
[d] *Department of Chemistry, University of Patras, Patras 26504, Greece*
[e] *Synthesis and Solid-State Pharmaceutical Centre (SSPC), School of Chemistry,*
   College of Science and Engineering, National University of Ireland Galway,
   University Road, Galway, H91 TK33, Ireland.
   E-mail: constantina.papatriantafyllopo@nuigalway.ie
† Electronic supplementary information (ESI) available: Experimental details, structural tables and figures and magnetism plots. CCDC 2071106 (**1**), 2071104 (**2**) and 2071105 (**3**). For ESI and crystallographic data in CIF or other electronic format see DOI: 10.1039/d1cc01815a
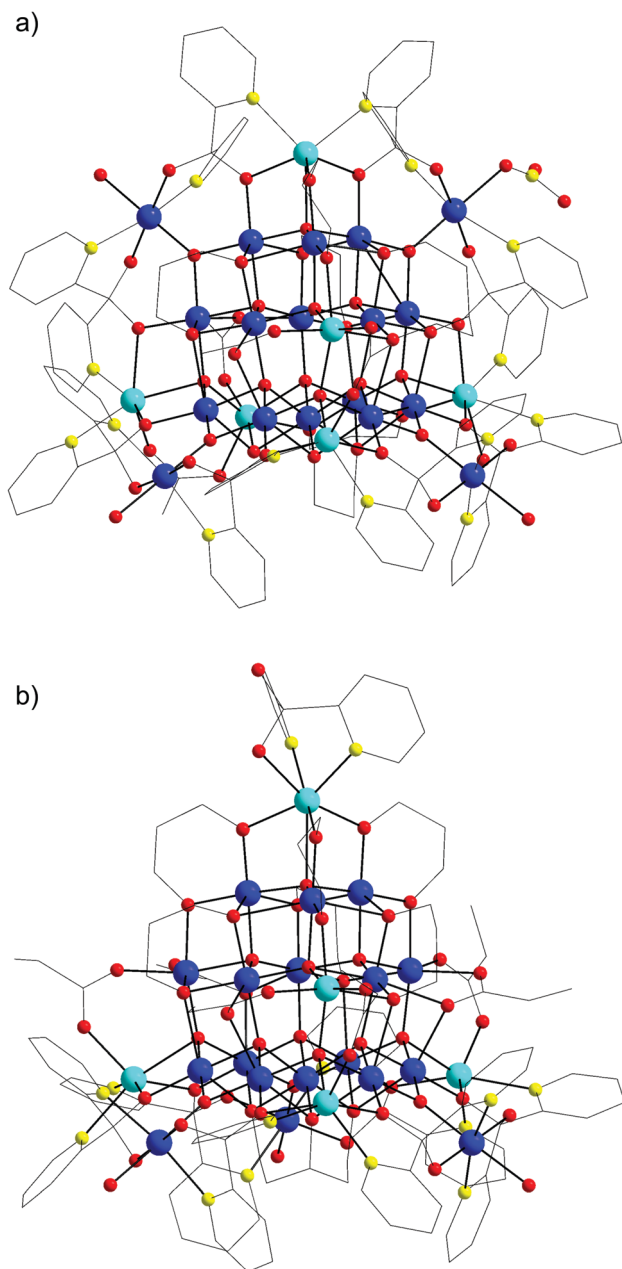
twenty, *etc.*, metal ions, respectively, and exhibit highly symmetric structures, with the highest nuclearity member known being a M$_{56}$ T6 cluster.[27] Similar supertetrahedral metal clusters possessing O^{2-}/OH$^-$/OR$^-$ ligands and transition metal ions at moderate oxidation states have also been reported. The most common among them is the T3 one that consists of ten metal ions. In fact, such decametallic supertetrahedra have appeared mainly in Mn carboxylate chemistry with the most common [Mn$^{III}_6$Mn$^{II}_4$(μ_4-O)$_4$]$^{18+}$ type usually exhibiting ferromagnetic exchange interactions, a large spin ground state value S_T = 22 and an enhanced magnetocaloric effect.[17–20] This structural core has also been found as a fragment in high nuclearity homo- and heterometallic clusters[7,29,30] with the largest one being a [Mn$_{49}$] cuboctahedron consisting of eight edge-sharing [Mn$^{III}_6$Mn$^{II}_4$(μ_4-O)$_4$]$^{18+}$ supertetrahedral sub-units,[30] often exhibiting entirely ferromagnetic interactions and giant S_T values, up to 83/2 in a Mn$_{19}$ cluster.[7] Although supertetrahedra T2 and T3 are well – known in 3d metal cluster chemistry, the higher nuclearity analogues are very uncommon[31] in contrast to the situation with metal chalcogenide compounds.

Herein, we report three new structurally related, high nuclearity clusters, [Mn$_{24}$O$_{14}$(OH)$_2$\{(py)$_2$CO$_2$\}$_8$(pd)$_6$(MeCO$_2$)$_4$(NO$_3$)$_{0.5}$(H$_2$O)$_{4.1}$] (NO$_3$)$_{1.3}$(OH)$_{2.2}$ (**1**) and [Mn$_{23}$O$_{13}$(OH)\{(py)$_2$C(O)$_2$\}$_6$(pd)$_7$(RCO$_2$)$_6$ (H$_2$O)$_{5.25}$(L)$_{0.25}n$](OH)$_{4.25}$(X)$_{0.75}$ (R = Me, L = H$_2$O, n = 3, X = OH$^-$ **2**; R = Et, L = (py)$_2$C(OH)$_2$, n = 1, X = NO$_3^-$ **3**), where (py)$_2$C(OH)$_2$ and (py)$_2$C(O)$_2$ are the neutral and dianionic forms of the gem-diol derivative of (py)$_2$CO, respectively, and pdH$_2$ is 1,3-propanediol. They were prepared from the combination of pdH$_2$ and (py)$_2$CO in reactions with Mn salts,[32] display supertetrahedral T4–based Mn/O structural cores and exhibit single–molecule magnetism (SMM) behaviour.

The reaction of Mn(NO$_3$)$_2$·4H$_2$O, pdH$_2$ and (py)$_2$CO in the presence of NEt$_3$ and MeCO$_2$Na in a molar ratio of ∼ 1:1.4:0.2:0.7:0.3 in EtOH eventually led to dark brown crystals of **1** after several weeks. Compound **1** crystallizes in the triclinic *P*1̄ space group and its molecular structure (Fig. 1a) contains a mixed-valent cluster cation based on a

Fig. 1   Representations of the molecular structures of compounds (a) **1** and (b) **3**. Colour code: Mn^{II}, turqoise; Mn^{III}, blue; O, red; N, yellow; C, grey. H atoms and the counter ions are omitted for clarity.

Fig. 2   Representations of the Mn/O^{2-} cores of compounds (a) **1** and (b) **2**, **3**. Colour code: Mn^{II}, turqoise; Mn^{III}, blue; O, red.

$[\text{Mn}^{III}_{18}\text{Mn}^{II}_{6}(\mu_4\text{-O})_{10}(\mu_3\text{-O})_4]^{38+}$ tetracapped supertetrahedral T4 structural core (Fig. 2a). The oxidation states of the Mn ions[33] and the protonation levels of the O atoms[34] of **1**, as well as of the other reported compounds, were determined by bond valence sum (BVS) calculations (Tables S2–S7 in ESI†), charge considerations and inspection of the bond lengths. The [Mn$_{20}$] supertetrahedron comprises three triangles stacked one above the other consisting of 10, 6 and 3 metal ions with the last Mn ion occupying an apex position. The Mn ions within each triangle and between neighboring ones are held together through 6/3/1 μ_4-O^{2-} ions located in the basal, middle and
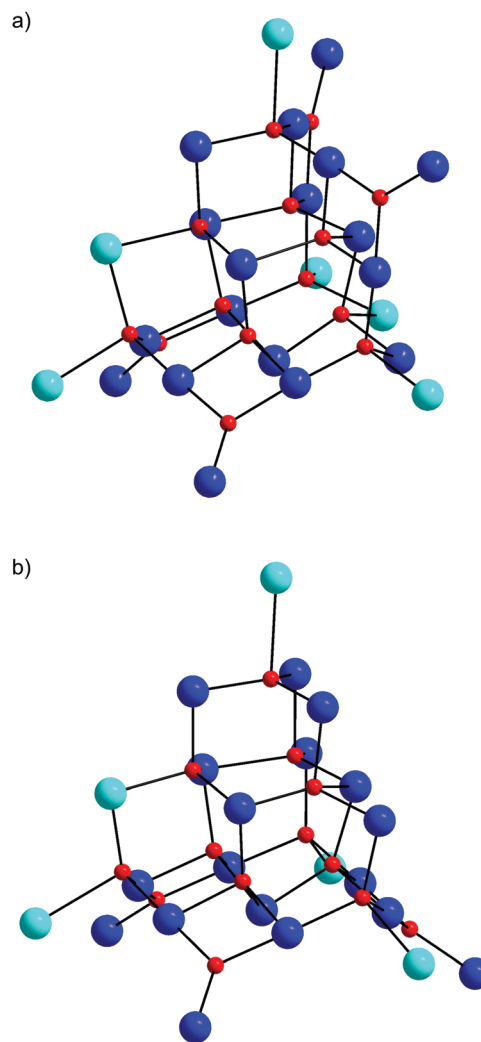
upper triangles, respectively, and four μ_3-O^{2-} ions bridging each edge of the supertetrahedron with a capping Mn^{3+} ion giving rise to the $[\text{Mn}^{III}_{18}\text{Mn}^{II}_{6}(\mu_4\text{-O})_{10}(\mu_3\text{-O})_4]^{38+}$ tetracapped-supertetrahedral T4 structural core. In addition, two μ_3-OH$^-$ ions located in the middle triangle connect it with the basal one. The Mn ions of the Mn$_{20}$ supertetrahedron are also linked through six pd^{2-}, four of which bridge in the η^3:η^3:μ_5 coordination mode and two in the η^2:η^2:μ_3 one, and four MeCO$_2^-$ groups bridging either in the common *syn*,*syn*-η^1:η^1:μ coordination mode (two of them) or in a η^2:η^1:μ_3 one (the remaining two). The vertices of the Mn$_{20}$ supertetrahedron are connected to the capping Mn^{III} ions through four pairs of η^1:η^2:η^1:η^1:μ_3 (py)$_2$C(O)$_2^{2-}$ ligands (Fig. S2, ESI†). The peripheral ligation of **1** is completed by terminal water molecules, one of which is disordered with a NO$_3^-$ anion.

Compound **2** was prepared from the same process as the one that yielded complex **1**, but with the use of a different solvent (MeCN instead of EtOH). Compound **2** (Fig. S4, ESI†) crystallizes in the cubic *Pa*3̄ space group and its molecular structure

contains a cationic cluster based on $[Mn_{23}(\mu_4\text{-O})_{10}(\mu_3\text{-O})_3]$ tricapped-supertetrahedral T4 structural core (Fig. 2b). The latter contains a $[Mn_{20}(\mu_4\text{-O})_{10}(\mu_3\text{-O})_3]^{29+}$ supertetrahedron, related to that of **1** discussed above, capped by three Mn^{III} ions attached *via* the three $\mu_3\text{-O}^{2-}$ to the three edges of the basal triangle. BVS calculations indicate some uncertainty in the determination of the oxidation state of Mn6 center (totally three symmetry – related ions) (Mn^{2+}: 2.60; Mn^{3+}: 2.38; Table S4, ESI†) whereas, a careful examination of the bond lengths revealed that they are shorter than the expected ones for Mn^{2+} oxidation state and longer for Mn^{3+} suggesting crystallographically-disordered mixed valency at this metal site.[35]

The isolation/crystallization of the propionate analogue was targeted and achieved from a similar synthetic procedure to the one for **2** except that $EtCO_2Na$ was used in place of $MeCO_2Na$ and the reaction took place in 2-propanol instead of MeCN. Compound **3** crystallizes in the trigonal $R\bar{3}$ space group and the molecular structure of the Mn_{23}-propionate cation (Fig. 1b) is related to that of **2**. BVS calculations (Table S6, ESI†) indicated a $[Mn^{III}_{18}Mn^{II}_5]$ oxidation state level and allowed the assignment of two of the Mn ions (Mn5 and Mn7) corresponding to the symmetry-equivalent Mn6 centers in **2** as Mn^{III} and the third one as Mn^{II} ion (Mn9) providing an evidence for a similar situation in **2**. The peripheral ligation in the $[Mn_{20}]$ super-tetrahedron is provided by three $\eta^2{:}\eta^2{:}\mu_3$ pd^{2-} and four $\eta^3{:}\eta^3{:}\mu_5$ pd^{2-} ligands as well as three $syn,syn\text{-}\eta^1{:}\eta^1{:}\mu$ and three $\eta^2{:}\eta^1{:}\mu_3$ propionate ligands. Each edge of the basal triangle of the $[Mn_{20}]$ supertetrahedron is connected to one capping Mn^{III} ion through a pair of $(py)_2C(O)_2^{2-}$ ligands (Fig. S8, ESI†) bridging in a $\eta^1{:}\eta^2{:}\eta^1{:}\eta^1{:}\mu_3$ mode leading to the $[Mn_{23}]$ aggregate. The peripheral ligation is completed by 0.25 $(py)_2C(OH)_2$ chelating one Mn^{II} ion disordered with 2.25 H_2O and three additional terminal H_2O molecules.

Compounds **1–3** thus exhibit related cores based on an unusual in 3d metal cluster chemistry supertetrahedron T4 (Fig. 2). In addition, they display very large dimensions as revealed from the sizes of the whole molecules and their Mn/O^{2-} cores which are about 2 nm and greater than 1 nm, respectively, in all cases. Notably, the combination of $(py)_2CO$ and pdH_2 led not only to one but to three different compounds based on this uncommon core. Another interesting feature highlighted from this study is the isolation from the same reaction but in different solvents of two metal clusters (**1**/**2** and **3**) differing slightly in nuclearity (Mn_{24} and Mn_{23}) and Mn/O core shape and topology (tetracapped *vs.* tricapped supertetrahedron T4). It is also interesting that the nuclearity of compounds **2** and **3** appears for the first time in Mn cluster chemistry.

Direct-current (dc) magnetic susceptibility (χ_M) measurements were performed on powdered crystalline samples of **1**·$22H_2O$–**3**·$28H_2O$ in the 5–300 K range in a 1 kG (0.1 T) magnetic field, and the data are plotted as $\chi_M T$ *vs.* T in Fig. 3a. The $\chi_M T$ for **1**·$22H_2O$, **2**·$33H_2O$ and **3**·$28H_2O$ decreases slowly from 57.18, 55.70 and 56.67 cm^3 mol^{-1} K at 300 K to 51.58, 50.29 and 48.86 at 100 K, and then rapidly to 30.14, 28.66 and 20.01 cm^3 mol^{-1} K, respectively, at 5 K. The 300 K values for

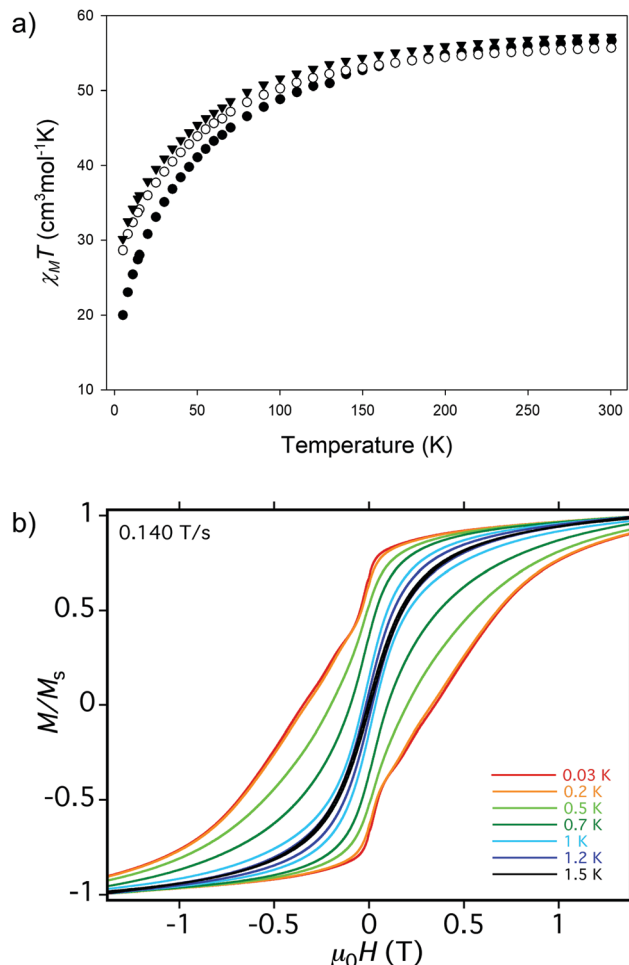Fig. 3 (a) $\chi_M T$ versus T plots for complexes **1**·$22H_2O$ (▼), **2**·$33H_2O$ (○) and **3**·$28H_2O$ (●) at 0.1 T and (b) magnetization (M) versus applied magnetic field ($\mu_0 H$) hysteresis loops for a single crystal of **1**·$2.5H_2O$·solvent at the indicated temperatures and a fixed field sweep rate of 0.140 T s^{-1}. The magnetization is normalized to its saturation value, M_S.

1·$22H_2O$–**3**·$28H_2O$ are lower than the spin-only ($g = 2$) values of 80.25 and 75.88 cm^3 mol^{-1} K for 18 Mn^{III}/6 Mn^{II} and 18 Mn^{III}/5 Mn^{II} non-interacting ions, respectively, indicating, together with the overall profiles of the $\chi_M T$ *versus* T plots, the presence of dominant antiferromagnetic exchange interactions between the metal ions. Variable field – variable temperature magnetization measurements were performed at applied magnetic fields and temperatures in the 1–70 kG and 1.8–10.0 K range, respectively, and the data are shown in Fig. S10–S12 in ESI,† as reduced magnetization ($M/N\mu_B$) *vs.* H/T plots, where M is the magnetization, N is Avogadro's number, μ_B is the Bohr magneton, and H is the magnetic field.

Alternating current (ac) magnetic susceptibility studies were also performed for the three compounds and the in-phase and out-of-phase data are shown in Fig. S13 (ESI†). Below ∼3.5 K, a frequency dependent decrease of the $\chi'_M T$ is observed followed by a concomitant increase of the χ''_M signals. This behaviour is indicative of the presence of slow relaxation of the magnetization vector suggesting that the compounds may be new SMMs.

This was confirmed from magnetization *versus* applied dc-field studies on single crystals at temperatures down to 0.03 K using a micro-SQUID apparatus. Hysteresis loops were seen below ~1.5 K whose coercivities increase with decreasing temperature and increasing field sweep rate (Fig. 3b and Fig. S14–S16, ESI†), as expected for superparamagnet-like behaviour, proving that they are new SMMs. The structural relation of the three compounds is clearly reflected to their magnetic properties which display a significant similarity. This includes the profiles of the $x_M T$ *vs. T* plots as well as the presence of frequency – dependent out-of-phase ac signals at $T < 3.5$ K and of hysteresis loops in magnetization *vs.* dc field scans below 1.5 K.

In conclusion, the combination of pdH$_2$ with (py)$_2$CO in Mn cluster chemistry has provided access to three new nanosized clusters and SMMs [[Mn$_{24}$] (**1**) and [Mn$_{23}$] (**2** and **3**)] with uncommon supertetrahedral T4 – like Mn/O cores. The present study establishes the employment of the ligands pdH$_2$ and (py)$_2$CO in Mn chemistry[32] as a fruitful source of polynuclear complexes with novel crystal structures and magnetic properties. It also shows that diols can lead to nanosized Mn clusters not only when they are employed as the main chelate[36] but also in combination with other well known chelates,[37] even bulky ones such as (py)$_2$CO. In fact, the isolated compounds are only slightly smaller than the [Mn$_{26}$] compounds which are the highest nuclearity M-(py)$_2$CO (M = any metal ion) clusters reported.[38–40] Further studies targeted at attaining more high nuclearity Mn/(py)$_2$CO/diol clusters are in progress and will be reported in due course.

Conflicts of interest

There are no conflicts to declare.

References

1 R. Bagai and G. Christou, *Chem. Soc. Rev.*, 2009, **38**, 1011.
2 C. J. Milios and R. E. P. Winpenny, *Struct. Bonding*, 2015, **164**, 1.
3 J. Ferrando-Soria, J. Vallejo, M. Castellano, J. Martinez-Lillo, E. Pardo, J. Cano, I. Castro, F. Lloret, R. Ruiz-Garcia and M. Julve, *Coord. Chem. Rev.*, 2017, **339**, 17.
4 D. Maniaki, E. Pilichos and S. P. Perlepes, *Front. Chem.*, 2018, **6**, 461.
5 K. S. Pedersen, J. Bendix and R. Clérac, *Chem. Commun.*, 2014, **50**, 4396.
6 T. C. Stamatatos and E. Rentschler, *Chem. Commun.*, 2019, **55**, 11.
7 A. M. Ako, I. J. Hewitt, V. Mereacre, R. Clerac, W. Wernsdorfer, C. E. Anson and A. K. Powell, *Angew. Chem., Int. Ed.*, 2006, **45**, 4926.
8 E. Coronado, *Nat. Rev. Mater.*, 2020, **5**, 87.
9 Y.-Z. Zheng, G.-J. Zhou, Z. Zheng and R. E. P. Winpenny, *Chem. Soc. Rev.*, 2014, **43**, 1462.
10 L. Bogani, *Struct. Bonding*, 2015, **164**, 331.
11 G. Aromí, D. Aguilà, P. Gamez, F. Luis and O. Roubeau, *Chem. Soc. Rev.*, 2012, **41**, 537.
12 J. Yano and V. Yachandra, *Chem. Rev.*, 2014, **114**, 4175.
13 Y.-K. Deng, H.-F. Su, J.-H. Xu, W.-G. Wang, M. Kurmoo, S.-C. Lin, Y.-Z. Tan, J. Jia, D. Sun and L.-S. Zheng, *J. Am. Chem. Soc.*, 2016, **138**, 1328.
14 B.-Q. Ji, H.-F. Su, M. Jagodic, Z. Jaglicic, M. Kurmoo, X.-P. Wang, C.-H. Tung, Z.-Z. Cao and D. Sun, *Inorg. Chem.*, 2019, **58**, 3800.
15 K. J. Mitchell, K. A. Abboud and G. Christou, *Nat. Commun.*, 2017, **8**, 1445.
16 K. J. Mitchell, J. L. Goodsell, B. Russell-Webster, U. T. Twahir, A. Angerhofer, K. A. Abboud and G. Christou, *Inorg. Chem.*, 2021, **60**, 1641.
17 M. Manoli, R. D. L. Johnstone, S. Parsons, M. Murrie, M. Affronte, M. Evangelisti and E. K. Brechin, *Angew. Chem., Int. Ed.*, 2007, **46**, 4456.
18 T. C. Stamatatos, K. A. Abboud, W. Wernsdorfer and G. Christou, *Angew. Chem., Int. Ed.*, 2006, **45**, 4134.
19 S. Nayak, M. Evangelisti, A. K. Powell and J. Reedijk, *Chem. – Eur. J.*, 2010, **16**, 12865.
20 G. Wu, J. Huang, L. Sun, J. Bai, G. Li, E. Cremades, E. Ruiz, R. Clérac and S. Qiu, *Inorg. Chem.*, 2011, **50**, 8580.
21 J. T. Brockman, J. C. Huffman and G. Christou, *Angew. Chem., Int. Ed.*, 2002, **41**, 2506.
22 I. L. Malaestean, A. Ellern and P. Kögerler, *Eur. J. Inorg. Chem.*, 2013, 1635.
23 A. B. Canaj, M. Siczek, T. Lis, M. Murrie, E. K. Brechin and C. J. Milios, *Dalton Trans.*, 2017, **46**, 7677.
24 A. E. Dearle, D. J. Cutler, H. W. L. Fraser, S. Sanz, E. Lee, S. Dey, I. F. Diaz-Ortega, G. S. Nichol, H. Nojiri, M. Evangelisti, G. Rajaraman, J. Schnack, L. Cronin and E. K. Brechin, *Angew. Chem., Int. Ed.*, 2019, **58**, 16903.
25 A. E. Thuijs, X.-G. Li, Y.-P. Wang, K. A. Abboud, X.-G. Zhang, H.-P. Cheng and G. Christou, *Nat. Commun.*, 2017, **8**, 500.
26 X. Bu, N. Zheng, Y. Li and P. Feng, *J. Am. Chem. Soc.*, 2002, **124**, 12646.
27 X. Xu, W. Wang, D. Liu, D. Hu, T. Wu, X. Bu and P. Feng, *J. Am. Chem. Soc.*, 2018, **140**, 888.
28 X. Bu, N. Zheng and P. Feng, *Chem. – Eur. J.*, 2004, **10**, 3356.
29 E. E. Moushi, T. C. Stamatatos, W. Wernsdorfer, V. Nastopoulos, G. Christou and A. J. Tasiopoulos, *Inorg. Chem.*, 2009, **48**, 5049.
30 M. Manoli, S. Alexandrou, L. Pham, G. Lorusso, W. Wernsdorfer, M. Evangelisti, G. Christou and A. J. Tasiopoulos, *Angew. Chem., Int. Ed.*, 2016, **55**, 679.
31 W. Du, Y.-L. Bai, X. Yin, J. Fang, S. Zhu and J. Tao, *Chem. – Eur. J.*, 2017, **23**, 8025.
32 M. Savva, K. Skordi, A. D. Fournet, A. E. Thuijs, G. Christou, S. P. Perlepes, C. Papatriantafyllopoulou and A. J. Tasiopoulos, *Inorg. Chem.*, 2017, **56**, 5657.
33 W. Liu and H. H. Thorp, *Inorg. Chem.*, 1993, **32**, 4102.
34 I. D. Brown and D. Altermatt, *Acta Crystallogr., Sect. B: Struct. Sci.*, 1985, **41**, 244.
35 H.-J. Lun, L. Xu, X.-J. Kong, L.-S. Long and L.-S. Zheng, *Inorg. Chem.*, 2021, **60**, 10079.
36 E. E. Moushi, C. Lampropoulos, W. Wernsdorfer, V. Nastopoulos, G. Christou and A. J. Tasiopoulos, *J. Am. Chem. Soc.*, 2010, **132**, 16146.
37 M. Manoli, R. Inglis, M. J. Manos, V. Nastopoulos, W. Wernsdorfer, E. K. Brechin and A. J. Tasiopoulos, *Angew. Chem., Int. Ed.*, 2011, **50**, 4441.
38 T. C. Stamatatos, V. Nastopoulos, A. J. Tasiopoulos, E. E. Moushi, W. Wernsdorfer, G. Christou and S. P. Perlepes, *Inorg. Chem.*, 2008, **47**, 10081.
39 T. C. Stamatatos, K. A. Abboud, W. Wernsdorfer and G. Christou, *Angew. Chem., Int. Ed.*, 2008, **47**, 6694.
40 T. C. Stamatatos, C. G. Efthymiou, C. C. Stoumpos and S. P. Perlepes, *Eur. J. Inorg. Chem.*, 2009, 3361.